

**Structural Polarity Induced by Cooperative Hydrogen Bonding and
Lone-Pair Alignment in the Molecular Uranyl Iodate, $\text{Na}_2[\text{UO}_2(\text{IO}_3)_4(\text{H}_2\text{O})]$**

Travis H. Bray,[†] James V. Beitz,[‡] Amanda C. Bean,[§] Yaqin Yu,[†]
and Thomas E. Albrecht-Schmitt^{†,*}

A Contribution from the [†]Department of Chemistry and Biochemistry,

and E. C. Leach Nuclear Science Center,

Auburn University, Auburn, Alabama 36849

[‡]Chemistry Division, Argonne National Laboratory, Argonne, Illinois 60439

[§]Nuclear Materials Technology Division, Los Alamos National Laboratory, Los Alamos,

New Mexico, 87545

A Revised Submission to Inorganic Chemistry

Abstract

$\text{Na}_2[\text{UO}_2(\text{IO}_3)_4(\text{H}_2\text{O})]$ has been synthesized under mild hydrothermal conditions. Its structure consists of Na^+ cations and $[\text{UO}_2(\text{IO}_3)_4(\text{H}_2\text{O})]^{2-}$ anions. The $[\text{UO}_2(\text{IO}_3)_4(\text{H}_2\text{O})]^{2-}$ anions are formed from the coordination of a nearly linear uranyl, UO_2^{2+} , cation by four monodentate IO_3^{1-} anions and a coordinating water molecule to yield a pentagonal bipyramidal environment around the uranium center. The water molecules form intermolecular hydrogen bonds with the terminal oxo atoms of neighboring $[\text{UO}_2(\text{IO}_3)_4(\text{H}_2\text{O})]^{2-}$ anions to yield one-dimensional chains that extend down the b axis. There are two crystallographically unique iodate anions in the structure of $\text{Na}_2[\text{UO}_2(\text{IO}_3)_4(\text{H}_2\text{O})]$. One of these anions is aligned so that the lone-pair of electrons is also directed along the b axis. The overall structure is therefore polar owing to the cooperative alignment of both the hydrogen bonds and the lone-pair of electrons on iodate. The polarity of the monoclinic space group $C2$ ($a = 11.3810(12)$ Å, $b = 8.0547(8)$ Å, $c = 7.6515(8)$ Å, $\beta = 90.102(2)^\circ$, $Z = 2$, $T = 193$ K) found for this compound is consistent with the structure. Second-harmonic generation of 532 nm light from a 1064 nm laser source yields a response of approximately $16\times \alpha\text{-SiO}_2$.

INTRODUCTION

Actinide iodates have been the subject of recent intense interest owing primarily to their rich structural chemistry. In the past six years, examples of Th,¹ U,² Np,³ Pu,^{3c,4} Am,⁵ Cm,⁶ and even Cf⁷ iodates have been reported. This family of compounds spans several themes in the area of f-block elements with oxoanions containing a nonbonding, but stereochemically active lone-pair of electrons. Some of these topics include the formation of noncentrosymmetric structures, a feature that is often ascribed to the alignment of the lone-pairs in the solid state,^{3c,3d,4a,5a} and the apparent excision of low-dimensional substructures from higher dimensional structure types.^{2f,2g} Both of these attributes can be identified in uranium, neptunium, and plutonium iodates. The early actinide iodates have thus far been isolated with the actinides in the +5 or +6 oxidation states, and therefore contain the requisite approximately linear dioxo actinyl cation, AnO₂ⁿ⁺ (An = U, Np, Pu; n = 1, 2).

In uranyl iodates, the lone-pair of electrons on I(V) can play a number of roles in both the local and extended structural chemistry. In general, the presence of a lone-pair of electrons on an oxoanion has been found to reduce the overall dimensionality from the layered forms that dominate uranyl solids,⁸ to one-dimensional chain and ribbon structures. This occurs in anhydrous uranyl iodate, UO₂(IO₃)₂,^{2b} as well more complex materials, such as Cs₂[(UO₂)₃Cl₂(IO₃)(OH)O₂].2H₂O,^{2c} Rb[(UO₂)(CrO₄)(IO₃)(H₂O)],^{2d} A₂[(UO₂)(MO₄)(IO₃)₂] (A = K, Rb, Cs; M = Cr, Mo),^{2d,2e} A₂[(UO₂)₃(IO₃)₄O₂] (A = K, Rb, Tl),^{2f,2g} AE[(UO₂)₂(IO₃)₂O₂] (AE = Sr, Ba, Pb),^{2f,2g} K₃[(UO₂)₂(IO₃)₆](IO₃)·H₂O,^{2h} and K[UO₂(IO₃)₃].^{2j} Until now, the creation of acentric structures ascribed to lone-pair alignment has been absent from uranyl iodate chemistry, but it is displayed in the Np(V) iodate, NpO₂(IO₃)₃,^{3d} and in An(VI) iodates, AnO₂(IO₃)₂·H₂O (An = Np, Pu).^{3c,4a} Herein we report the preparation and characterization of

the first zero-dimensional, or molecular, uranyl iodate, $\text{Na}_2[\text{UO}_2(\text{IO}_3)_4(\text{H}_2\text{O})]$. This compound adopts a polar structure owing to cooperative alignment of both hydrogen bonds from coordinated water molecules and the lone-pairs of electrons on the iodate anions.

EXPERIMENTAL

Syntheses. $\text{UO}_2(\text{NO}_3)_2 \cdot 6\text{H}_2\text{O}$ (98%, Alfa-Aesar), UO_3 (99.8%, Alfa-Aesar), 2,2'-Bipyridyl (99%, Alfa-Aesar), I_2O_5 (98%, Alfa-Aesar), NaCl (99%, Alfa-Aesar), HCl (37.4%, Fisher Scientific), and NaHCO_3 (99%, Alfa Aesar) were used as received. Reactions were run in PTFE-lined Parr 4749 autoclaves with a 23 mL internal volume. Distilled and Millipore filtered water with a resistance of 18.2 $\text{M}\Omega\text{-cm}$ was used in all reactions. Standard precautions were performed for handling radioactive materials during work with $\text{UO}_2(\text{NO}_3)_2 \cdot 6\text{H}_2\text{O}$, UO_3 , and the products of the reactions. Semi-quantitative EDX analyses were performed using a JEOL 7000F field emission SEM. Na, U, and I percentages were calibrated against standards.

$\text{Na}_2[\text{UO}_2(\text{IO}_3)_4(\text{H}_2\text{O})]$ (Method 1). $\text{UO}_2(\text{NO}_3)_2 \cdot 6\text{H}_2\text{O}$ (82.8 mg, 0.165 mmol), I_2O_5 (175.4 mg, 0.525 mmol), 2,2'-bipyridyl (32.8 mg, 0.210 mmol), HCl (0.05 mL, 0.018 mmol), NaHCO_3 (132.4 mg, 1.58 mmol), and 1.5 mL of water were loaded into a 23 mL autoclave. The autoclave was sealed and heated to 120 °C in a box furnace for 7 d. The autoclave was then cooled at an average rate of 9 °C/h to room temperature. The product consisted of yellow crystals ranging in habit from small rectangular plates to nearly cubic prisms, all of which were $\text{Na}_2[\text{UO}_2(\text{IO}_3)_4(\text{H}_2\text{O})]$. The product was thoroughly washed with water, then rinsed with methanol, and allowed to dry. Yield, 153 mg (90% based on U). EDX analysis provided Na:U:I ratio of approximately 2:1:4. IR (KBr, cm^{-1}) vibrational bands are given in Table 1.⁹ A X-ray powder diffraction pattern was measured and compared to a powder pattern generated from

single crystal X-ray diffraction data using the ATOMS program. These data show that $\text{Na}_2[\text{UO}_2(\text{IO}_3)_4(\text{H}_2\text{O})]$ is the only crystalline phase present in the solid (see Supporting Information).

$\text{Na}_2[\text{UO}_2(\text{IO}_3)_4(\text{H}_2\text{O})]$ (Method 2). UO_3 (114.9 mg, 0.4017 mmol), I_2O_5 (267.9 mg, 0.8026 mmol), NaCl (117.3 mg, 2.0071 mmol), and 0.5 mL of water were loaded into a 23 mL autoclave. The autoclave was sealed and heated to 180 °C in a box furnace for 3 d. The autoclave was then cooled at an average rate of 9 °C/h to room temperature. The product consisted of yellow crystals of $\text{Na}_2[\text{UO}_2(\text{IO}_3)_4(\text{H}_2\text{O})]$. The product was thoroughly washed with water, then rinsed with methanol, and allowed to dry. Powder X-ray diffraction data were used to confirm product purity. Yield, 362 mg (87% based on U).

Crystallographic Studies. A single crystal of $\text{Na}_2[\text{UO}_2(\text{IO}_3)_4(\text{H}_2\text{O})]$ with dimensions of 0.128 x 0.124 x 0.082 mm, was mounted on a glass fiber and optically aligned on a Bruker APEX CCD X-ray diffractometer using a digital camera. Initial intensity measurements were performed using graphite monochromated Mo $\text{K}\alpha$ radiation from a sealed tube and monocapillary collimator. SMART (v 5.624) was used for preliminary determination of the cell constants and data collection control. The intensities of reflections of a sphere were collected by a combination of 3 sets of exposures (frames). Each set had a different ϕ angle for the crystal and each exposure covered a range of 0.3° in ω . A total of 1800 frames were collected with an exposure time per frame of 30 s.

For $\text{Na}_2[\text{UO}_2(\text{IO}_3)_4(\text{H}_2\text{O})]$, determination of integrated intensities and global refinement were performed with the Bruker SAINT (v 6.02) software package using a narrow-frame integration algorithm. These data were treated with a semi-empirical absorption correction by SADABS.¹⁰ The program suite SHELXTL (v 6.12) was used for space group determination

(XPREP), direct methods structure solution (XS), and least-squares refinement (XL).¹¹ The final refinements included anisotropic displacement parameters for all atoms. Secondary extinction was not noted. Crystals of $\text{Na}_2[\text{UO}_2(\text{IO}_3)_4(\text{H}_2\text{O})]$ crystallize in the polar monoclinic space group $C2$. The crystal used for these X-ray diffraction experiments proved to be an enantiomorphic twin with a Flack parameter of 0.459(7). Missed symmetry was checked for using the ADDSYMM and NEWSYMM programs that are a part of the PLATON package.¹² This was particularly important because the suspiciously small β angle of $90.102(2)^\circ$ is often a cause of twinning and pseudo-orthorhombic symmetry – neither were detected. Some crystallographic details are given in Table 2. Additional details can be found in the Supporting Information.

Nonlinear Optical Measurements. Powder second-harmonic generation (SHG) measurements were performed on a Kurtz-Perry nonlinear optical system¹³ as modified by Porter and coworkers,¹⁴ and updated here to include laser pulse energy normalization. A Q-switched Nd:YAG laser (Continuum Surelite I-10), operated at 10 Hz, provided the 1064 nm light used for all measurements. The SHG intensity was recorded from 60 mg of $\text{Na}_2[\text{UO}_2(\text{IO}_3)_4(\text{H}_2\text{O})]$ and from fine ground α -quartz (crystalline SiO_2). These powders were placed in separate glass tubes of the same dimensions. No index of refraction matching fluid was used in these experiments. The SHG light at 532 nm was collected in reflection, selected by a narrow band-pass interference filter (Pomfret) and detected by a photomultiplier tube (RCA 1P28). A near normal incidence beam splitter reflected a small fraction of the laser beam onto a pyroelectric detector (Molelectron J3-05) that was used as a laser pulse energy monitor. A digital storage oscilloscope (Tektronix TDS 640A) signal averaged and recorded both the SHG and incident laser energy signals. Average laser power was measured separately with a calibrated Scientech volume absorber calorimeter. The observed SHG intensity per unit laser intensity, $I^{2\omega}$, was obtained by dividing

the SHG signal by the laser energy signal. Replicate measurements determined the value of interest for the sample compound, $I^{2\omega}$ (s), and for α -quartz, $I^{2\omega}$ (q). The ratio of these values, $I^{2\omega}$ (s) / $I^{2\omega}$ (q), was found to be 16 at an incident laser intensity of 17 MW/cm².

Thermal Analysis. Thermal data for Na₂[UO₂(IO₃)₄(H₂O)] were collected using a TA Instruments, Model 2920 Differential Scanning Calorimeter (DSC) and a TA Q50 Thermogravimetric Analyzer (TGA). Samples (~10 mg) were encapsulated in aluminum or platinum pans and heated at 10 °C/min from 25 °C to 600 °C (DSC) and from 25 °C to 400 °C (TGA) under a nitrogen atmosphere.

Powder X-ray Diffraction. Powder X-ray diffraction patterns were collected with a Rigaku Miniflex powder X-ray diffractometer using Cu K α ($\lambda = 1.54056 \text{ \AA}$) radiation.

RESULTS AND DISCUSSION

Synthesis. The synthesis of Na₂[UO₂(IO₃)₄(H₂O)] differs from that of most uranyl iodates in that the pH was intentionally increased through the addition of both bicarbonate and 2,2'-bipyridyl. Both the bicarbonate and 2,2'-bipyridyl are sacrificial, because the former is decomposed by the acidic conditions, and the latter is subject to both oxo atom transfer (oxidation) and iodination by the iodate anion under these conditions.¹⁵ The initial pH of the mixture is approximately 1.3, but increases to 4.1 over the course of the reaction, resulting in the formation of single crystals of Na₂[UO₂(IO₃)₄(H₂O)] (Method 1). We have found that the crystallinity of the product can be substantially improved through the addition of a few drops of conc. HF to the initial reaction mixture. Alternatively, Na₂[UO₂(IO₃)₄(H₂O)] can be prepared in a straightforward manner by reacting NaCl with UO₃ and I₂O₅ under hydrothermal conditions (Method 2). Using this method the average size of crystals steadily increases as the amount of

water is decreased from 3 to 1 to 0.5 mL. From of an ease of synthesis standpoint, this second preparation is somewhat preferable. However, the crystals that we have grown using Method 2 have been twinned.

Structural Features of Na₂[UO₂(IO₃)₄(H₂O)]. The structure of Na₂[UO₂(IO₃)₄(H₂O)] is distinct from all previously reported actinyl iodates in that it consists of Na⁺ cations and [UO₂(IO₃)₄(H₂O)]²⁻ anions. This is the first molecular actinide iodate. Molecular iodates containing metals are rare in general, being known only from [CrO₃(IO₃)]¹⁻,¹⁶ [MoO₂(IO₃)₄]²⁻,¹⁷ and [M(IO₃)₆]²⁻ (M = Ti,¹⁸ Zr,¹⁹ Mo¹⁹). An important comparison to be made is between the [MoO₂(IO₃)₄]²⁻ and [UO₂(IO₃)₄(H₂O)]²⁻ anions. In the former Mo(VI) compound, the well-known *cis*-MoO₂²⁺ cation exists, and owing to second-order Jahn-Teller effects,²⁰ the Mo atom is distorted far from idealized octahedral symmetry. In contrast, the U(VI) compound contains the *trans*-UO₂²⁺ cation. The four iodate anions bind this cation perpendicular to the uranyl axis through a single oxo atom from the iodate anions. The fifth site in the pentagonal plane is occupied by a water molecule. The [UO₂(IO₃)₄(H₂O)]²⁻ anion has two-fold symmetry as is depicted in Figure 1. The short U=O bond distances of 1.787(6) Å are typical for uranyl compounds, as is the approximately linear O–U–O angle of 179.2(6)°.²¹ The U–O distances to the iodate anions are 2.302(8) and 2.345(7) Å. The longest U–O distance is to the coordinated water molecule with a distance of 2.450(11) Å. This distance is similar to that found between the water molecule and the uranyl cation (2.458(5) Å) in UO₂(IO₃)₂(H₂O).^{2b} Furthermore, it should be noted that the [UO₂(IO₃)₄(H₂O)]²⁻ anion is the basic building unit found in layered structure of UO₂(IO₃)₂(H₂O) as shown in Figure 2.^{2b} Bond-valence sum calculations^{22,23} using the parameters for seven coordinate U(VI) given by Burns et al. yield a value of 6.09,²¹ which is consistent with this compound containing hexavalent uranium.

I–O distances within the iodate anions can be roughly correlated with their binding mode. The I–O distances observed where one of the oxygen atoms is involved in bonding to the uranium atom are slightly longer than the terminal ones. In the iodate anions containing I(1), the terminal I–O distances are 1.795(7) and 1.799(7) Å, whereas the bridging oxo atom has a bond distance of 1.843(7). The same pattern is observed for I(2) with terminal distances of 1.793(7) and 1.803(7) Å, and bridging distance of 1.811(7) Å. Here the bond distance variations are not statistically significant. Bond-valence sums for I(1) and I(2) are 4.99 and 5.12, respectively.^{22,23} These bond-valences are consistent with I(V). Selected bond distances and angles are given in Table 3.

Na₂[UO₂(IO₃)₄(H₂O)] further deviates from previously known uranyl iodates in that the structure is polar. Polarity in actinyl iodates has been previously observed in AnO₂(IO₃)₂·H₂O (An = Np, Pu)^{3c,4a} and NpO₂(IO₃)₃^d wherein the iodate anions are all aligned so that the lone-pair of electrons are directed along a single crystallographic axis. Similar alignment is also observed in the structure of Na₂[UO₂(IO₃)₄(H₂O)] where each of the crystallographically unique iodate units in the [UO₂(IO₃)₄(H₂O)]²⁻ anion is aligned along the *b* axis, as is shown in Figure 3. Owing to translational symmetry all of the [UO₂(IO₃)₄(H₂O)]²⁻ anions are therefore aligned in the same manner in the overall structure. The oddity of this observation is that because the iodate anions are monodentate, they should be able to freely rotate in solution, and, at first glance, there is no obvious reason for alignment in the solid state. However, as will become clear, there are a series of intermolecular interactions that account for the lone-pair alignment.

One of the key features of the structure of Na₂[UO₂(IO₃)₄(H₂O)] is that all of the water molecules are oriented so that they lie along the *b* axis. There are short O···O intermolecular contacts of 2.762(7) Å that are of appropriate length for hydrogen bonding between the water

molecule of one $[\text{UO}_2(\text{IO}_3)_4(\text{H}_2\text{O})]^{2-}$ anion and the neighboring terminal oxo atoms of the iodate anions in an adjacent anion. As can be seen in Figure 3, the hydrogen bonds yield one-dimensional chains that extend down the b axis. These hydrogen bonds orient one of the crystallographically unique iodate anions (I(2)). The second iodate anion, containing I(1), is more strongly aligned along the b axis than the I(2) iodate anion. Its alignment can be ascribed to intramolecular I...O interactions between iodate molecules in the anion, as depicted in Figure 3. This interaction is on the order of $2.827(7)$ Å, and is typical for intermolecular iodate contacts.^{2b,2f,2g,24-26} Therefore, the cooperative coexistence of hydrogen bonds and intermolecular iodate...iodate interactions leads to lone-pair alignment that contributes to the short- and long-range polarity in the structure of $\text{Na}_2[\text{UO}_2(\text{IO}_3)_4(\text{H}_2\text{O})]$.

The environments around the Na^+ cations must also contribute to the acentricity of the overall structure of $\text{Na}_2[\text{UO}_2(\text{IO}_3)_4(\text{H}_2\text{O})]$. There are two crystallographically unique Na^+ cations in this structure. Na(1) forms eight contacts ranging from $2.415(7)$ to $2.992(11)$ Å, with surrounding oxygen atoms to yield an approximately dodecahedral environment, as is shown in Figure 4a. The Na(1) center is shifted from the center of this unit toward one side by approximately 0.33 Å. Na(2) has six interactions with distances occurring from $2.303(6)$ to $2.343(9)$ Å to yield a distorted octahedral geometry, as depicted in Figure 4b. The environments around the Na^+ cations are also consistent with a polar structure. A packing diagram for $\text{Na}_2[\text{UO}_2(\text{IO}_3)_4(\text{H}_2\text{O})]$ is shown in Figure 5.

Structural-Property Relationships in $\text{Na}_2[\text{UO}_2(\text{IO}_3)_4(\text{H}_2\text{O})]$. A consequence of the polarity of $\text{Na}_2[\text{UO}_2(\text{IO}_3)_4(\text{H}_2\text{O})]$ is that it should be capable of second-harmonic generation (SHG) of laser light. SHG measurements have been made on many alkali metal, transition metal, and lanthanide iodates yielding a wide range of efficiencies that maximize with values as

large as $500\times$ α -quartz for $\text{Cs}[(\text{VO})_2(\text{IO}_3)_3\text{O}_2]$.^{27,28} For true quantification of the SHG response, the compounds must be ground into powders and sieved into ranges of particles sizes so that comparisons can be made between the compound in question and a standard using particles in the same size range. Measurements on sieved powders also allows one to determine whether or not the material is Type 1 or Type 2 phase-matchable. While this can be done with relative ease on non-radioactive material, the grinding and, more importantly, the sieving process, disperses fine particles making this procedure unsafe from a contamination standpoint. Therefore, we only make measurements on unsieved powders with radioactive material. The SHG response for the frequency doubling of 1064 nm laser light from a Nd:YAG laser to 532 nm light by $\text{Na}_2[\text{UO}_2(\text{IO}_3)_4(\text{H}_2\text{O})]$ was measured on unsieved powders to yield a small response of approximately $16\times$ α - SiO_2 . The observation of SHG from this material provides external confirmation of the polarity of the structure.

Thermal Behavior. The thermal stability of $\text{Na}_2[\text{UO}_2(\text{IO}_3)_4(\text{H}_2\text{O})]$ was investigated to address two issues. First, does the loss of coordinated water result in substantial structural changes? For example, the removal of water potentially opens a coordination site that the terminal oxo atoms of iodate anions from neighboring complexes might fill, thereby interconnecting $[\text{UO}_2(\text{IO}_3)_4]$ units into a structure of higher dimensionality. Second, what is the overall stability of a molecular uranyl iodate in comparison with the layered uranyl iodate $\text{UO}_2(\text{IO}_3)_2(\text{H}_2\text{O})$, which contains similar uranyl iodate hydrate building units? A DSC thermogram of $\text{Na}_2[\text{UO}_2(\text{IO}_3)_4(\text{H}_2\text{O})]$ reveals a complex series of endotherms beginning at 380 °C, as is shown in Figure 6. This large endotherm is followed by small events at 409, 424, and 492 °C, which precede a large multi-component endotherm centered at 543 °C. When combined with TGA data, it was determined that the first endotherm corresponds to water loss.

Water loss occurs from $\text{UO}_2(\text{IO}_3)_2(\text{H}_2\text{O})$ at 327 °C, and is not followed by any events until 572 °C, at which point iodate disproportionation takes place.^{2b} This is similar to the disproportionation temperature of $\text{Na}_2[\text{UO}_2(\text{IO}_3)_4(\text{H}_2\text{O})]$ as well as other actinide iodates such as $\text{Th}(\text{IO}_3)_2(\text{SeO}_4)(\text{H}_2\text{O})_3 \cdot \text{H}_2\text{O}$ and $\text{Th}(\text{CrO}_4)(\text{IO}_3)_2$, which undergo disproportionation at 537 °C and 543 °C, respectively.^{27d} It is of interest to note that if there are multiple crystallographically unique iodate anions, then multiple disproportionation events are often observed, as is the case for $\text{Na}_2[\text{UO}_2(\text{IO}_3)_4(\text{H}_2\text{O})]$. Although in this case, multiple iodate decompositions might be caused by the presence of a complex mixture that results from water loss and partial structural reorganization. The endothermic events between 409 and 492 °C may indeed correspond to the formation of novel uranyl iodate structures, but they are unfortunately located too closely to the iodate decomposition temperature for further investigation.

CONCLUSIONS

In this report we have demonstrated that the first molecular uranyl iodate can be prepared and crystallized in high yield by several methods. Concomitant formation of intermolecular hydrogen bonds and iodate...iodate interactions align the lone-pair of electrons on the iodate anions to yield a polar structure. This is also the first polar uranyl iodate.

One key issue that this and previous studies² indicate is that the alkali, alkaline-earth, and main group cations influence what kind of products can be isolated, i.e. they play different structure-directing roles despite all having the same shape. Table 4 provides a list of uranyl iodates for which single crystal structures are currently known. Factors that we have identified that can potentially alter the formation of different uranyl iodates are cation size, cation size to charge ratio, and the pH of the reaction mixture. When all other conditions are held as constant

as possible, we have found substantial changes in structure and composition at the $\text{Na}^+(\text{K}^+, \text{Rb}^+, \text{Tl}^+)|\text{Cs}^+$ boundaries in some systems. While K^+ , Rb^+ , and Tl^+ all yield the same uranyl iodate architecture in $\text{A}_2[(\text{UO}_2)_3(\text{IO}_3)_4\text{O}_2]$ ($\text{A} = \text{K}, \text{Rb}, \text{Tl}$),^{2f,2g} we have been unable to isolate the Cs^+ analog of these compounds despite repeated attempts over the years; instead $\text{Cs}_2[(\text{UO}_2)_3\text{Cl}_2(\text{IO}_3)(\text{OH})\text{O}_2]\cdot 2\text{H}_2\text{O}$ crystallizes from reactions with high CsCl concentrations.^{2c} As can be seen from this tabulation K^+ , Rb^+ , and Tl^+ are all similar in size, and result in the formation of the same inorganic ribbons. In this present work we observe that the presence of the small Na^+ cation allows for the synthesis of a uranyl iodate anion that we have yet to isolate from reactions with different cations. Na^+ is substantially smaller, and Cs^+ is substantially larger than K^+ , Rb^+ , and Tl^+ . We can not neglect that the different hydration energies of these cations could also alter the course of these reactions. The effects of the cation size to charge ratio are illustrated by K^+ and Ba^{2+} , which while similar in size, yield substantially different uranyl iodate architectures. When the cation is held constant, the pH of the reaction can substantially change the products that crystallize. For example, at low pH (~ 1) $\text{K}_2[(\text{UO}_2)_3(\text{IO}_3)_4\text{O}_2]$,^{2f,2g} crystallizes. As the pH is increased, $\text{K}[\text{UO}_2(\text{IO}_3)_3]^{2j}$ and $\text{K}_3[(\text{UO}_2)_2(\text{IO}_3)_6](\text{IO}_3)\cdot \text{H}_2\text{O}^{2h}$ can be isolated. It will be interesting to observe the effects of Li^+ in this regard because it should form stronger interactions with the surrounding oxygen-containing network than the heavier alkali metals cations.

Acknowledgment. This work was supported by the Chemical Sciences, Geosciences and Biosciences Division, Office of Basic Energy Sciences, Office of Science, Heavy Elements Program, U.S. Department of Energy under Grant DE-FG02-01ER15187, by the Office of Civilian Radioactive Waste Management, Office of Science and Technology and International,

through a subcontract with Argonne National Laboratory, and under Contract W-31-109-ENG-38 at Argonne National Laboratory.

Supporting Information Available: X-ray crystallographic file in CIF format, and powder X-ray diffraction data for $\text{Na}_2[\text{UO}_2(\text{IO}_3)_4(\text{H}_2\text{O})]$. This material is available free of charge via the Internet at <http://pubs.acs.org>.

References

- 1) a) Sullens, T. A.; Almond, P. M.; Byrd, J. A.; Beitz, J. V.; Bray, T. H.; Albrecht-Schmitt, T. E. *J. Solid State Chem.* **2006**, *179*, 1192. b) Sullens, T. A.; Almond, P. M.; Albrecht-Schmitt, T. E., *Mater. Res. Soc.*, **2006**, *893*, 283.
- 2) a) Weigel, F.; Engelhardt, L. W. H. *J. Less-Common Met.* **1983**, *91*, 339. b) Bean, A. C.; Peper, S. M.; Albrecht-Schmitt, T. E. *Chem. Mater.* **2001**, *13*, 1266. c) Bean, A. C.; Xu, Y.; Danis, J. A.; Albrecht-Schmitt, T. E.; Runde, W. *Inorg. Chem.* **2002**, *41*, 6775. d) Sykora, R. E.; McDaniel, S. M.; Wells, D. M.; Albrecht-Schmitt, T. E. *Inorg. Chem.* **2002**, *41*, 5126. e) Sykora, R. E.; Wells, D. M.; Albrecht-Schmitt, T. E. *Inorg. Chem.* **2002**, *41*, 2304. f) Bean, A. C.; Albrecht-Schmitt, T. E. *J. Solid State Chem.* **2001**, *161*, 416. g) Bean, A. C.; Ruf, M.; Albrecht-Schmitt, T. E. *Inorg. Chem.* **2001**, *40*, 3959. h) Sykora, R. E.; Bean, A. C.; Scott, B. L. Runde, W.; Albrecht-Schmitt, T. E. *J. Solid State Chem.* **2004**, *177*, 725. i) Bean, A. C.; Campana, C. F.; Kwon, O.; Albrecht-Schmitt, T. E. *J. Am. Chem. Soc.* **2001**, *123*, 8806. j) Shvareva, T. Y.; Almond, P. M.; Albrecht-Schmitt, T. E. *J. Solid State Chem.* **2005**, *178*, 499.
- 3) a) Bean, A. C.; Scott, B. L.; Albrecht-Schmitt, T. E.; Runde, W. *J. Solid State Chem.* **2004**, *176*, 1346. b) Sykora, R. E.; Bean, A. C.; Scott, B. L.; Runde, W.; Albrecht-Schmitt, T. E. *J. Solid State Chem.* **2004**, *177*, 725. c) Bean, A. C.; Scott, B. L.; Albrecht-Schmitt, T. E.; Runde, W. *Inorg. Chem.* **2003**, *42*, 5632. d) Albrecht-Schmitt, T. E.; Almond, P. M.; Sykora, R. E. *Inorg. Chem.* **2003**, *42*, 3788.
- 4) a) Runde, W.; Bean, A. C.; Albrecht-Schmitt, T. E.; Scott, B. L. *Chem. Commun.* **2003**, *4*, 478. b) Bean, A. C.; Abney, K.; Scott, B. L.; Runde, W. *Inorg. Chem.* **2005**, *44*, 5209.

- 5) a) Runde, W.; Bean, A. C.; Scott, B. L. *Chem. Commun.* **2003**, *15*, 1848. b) Sykora, R. E.; Assefa, Z.; Haire, R. G.; Albrecht-Schmitt, T. E. *Inorg. Chem.* **2005**, *44*, 5667. c) Runde, W.; Bean, A. C.; Brodnax, L. F.; Scott, B. L. *Inorg. Chem.* **2006**, *45*, 2479.
- 6) Sykora, R. E.; Assefa, Z.; Haire, R. G.; Albrecht-Schmitt, T. E. *J. Solid State Chem.* **2004**, *177*, 4413.
- 7) Sykora, R. E.; Assefa, Z.; Albrecht-Schmitt, T. E.; Haire, R. G. *Inorg. Chem.* **2006**, *45*, 475.
- 8) a) P. C. Burns, M. L. Miller, R. C. Ewing, *Can. Mineral.* **1996**, *34*, 845. b) P. C. Burns, In *Uranium: Mineralogy, Geochemistry and the Environment*; Burns, P. C.; Finch, R., Eds. Ch. 1, Mineralogical Society of America: Washington, DC, 1999. c) P. C. Burns, *Mater. Res. Soc. Symp. Proc.* **2004**, *802*, 89. d) Burns, P. C. *Can. Mineral.* **2005**, *43*, 1839.
- 9) a) Pracht, G.; Lange, N.; Lutz, H. D. *Thermochim. Acta* **1997**, *293*, 13. b) Lutz, H. D.; Alici, E.; Kellersohn, Th. *J. Raman Spectrosc.* **1990**, *21*, 387. b) Schellenschlager, V.; Pracht, G.; Lutz, H. D. *J. Raman Spectrosc.* **2001**, *32*, 373. c) Lutz, H. D.; Suchanek, E. *Spectrochim. Acta* **2000**, *A56*, 2707. d) Pracht, G.; Nagel, R.; Suchanek, E.; Lange, N.; Lutz, H. D. *Z. Anorg. Allg. Chem.* **1998**, *624*, 1355. e) Kellersohn, Th.; Alici, E.; Eber, D.; Lutz, H. D. *Z. Kristallogr.* **1993**, *203*, 225.
- 10) Sheldrick, G. M. *SADABS* 2001, Program for absorption correction using SMART CCD based on the method of Blessing; Blessing, R. H. *Acta Crystallogr.* **1995**, *A51*, 33.
- 11) Sheldrick, G. M. *SHELXTL* PC, Version 6.12, An Integrated System for Solving, Refining, and Displaying Crystal Structures from Diffraction Data; Siemens Analytical X-Ray Instruments, Inc.: Madison, WI 2001.

- 12) Spek, A. L. *Acta Crystallogr.* **1990**, *A46*, C34.
- 13) Kurtz, S. K.; Perry, T. T. *J. Appl. Phys.* **1968**, *39*, 3798.
- 14) Porter, Y.; Ok, K. M.; Bhuvanesh, N. S. P.; Halasyamani, P. S. *Chem. Mater.* **2001**, *13*, 1910.
- 15) Bray, T. H.; Albrecht-Schmitt, T. E. *unpublished results*.
- 16) Lofgren, P. *Acta Chem. Scand.* **1967**, *21*, 2781.
- 17) Sykora, R. E.; Wells, D. M.; Albrecht-Schmitt, T. E. *J. Solid State Chem.* **2002**, *166*, 442.
- 18) Ok, K. M.; Halasyamani, P. S. *Inorg. Chem.* **2005**, *44*, 2263.
- 19) Shehee, T. C.; Pehler, S. F.; Albrecht-Schmitt, T. E. *J. Alloys Compd.* **2005**, *388*, 225.
- 20) a) Opik, U.; Pryce, M. H. L.; *Proc. R. Soc. (London)* **1937**, *A161*, 220. b) Wheeler, R. A.; Whangbo, M. H.; Hughbanks, T.; Hoffman, R.; Burdett, J. K.; Albright, T. A. *J. Am. Chem. Soc.* **1986**, *108*, 2222. c) Pearson, R. G. *J. Mol. Struct.* **1983**, *103*, 25. d) Kang, S. K.; Tang, H.; Albright, T. A. *J. Am. Chem. Soc.* **1993**, *115*, 1971. e) Cohen, R. E. *Nature* **1992**, *358*, 136. f) Burdett, J. K. *Molecular Shapes*. Wiley-Interscience, New York, 1980. g) Kunz, M.; Brown, I. D. *J. Solid State Chem.* **1995**, *115*, 395. h) Goodenough, J. B.; Longo, J. M.: *Crystallographic and magnetic properties of perovskite and perovskite-related compounds*. In *Landolt-Bornstein*; Hellwege, K. H.; Hellwege, A. M., Eds.; Springer-Verlag: Berlin, 1970; Vol.4, pp 126-314. i) Brown, I. D. *Acta Crystallogr.* **1977**, *B33*, 1305.
- 21) Burns, P. C.; Ewing, R. C.; Hawthorne, F. C. *Can. Mineral.* **1997**, *35*, 1551.
- 22) Brown, I. D.; Altermatt, D. *Acta Crystallogr.* **1985**, *B41*, 244.
- 23) Brese, N. E.; O’Keeffe, M. *Acta Crystallogr.* **1991**, *B47*, 192.

- 24) Abrahams, S. C.; Bernstein, J. L.; Elemans, J. B. A. A.; Verschoor, G. C. *J. Chem. Phys.* **1973**, *59*, 2007.
- 25) Burns, P. C.; Hawthorne, F. C. *Can. Mineral.* **1993**, *31*, 313.
- 26) Cooper, M. A.; Hawthorne, F. C.; Roberts, A. C.; Grice, J. D.; Stirling, J. A. R.; Moffatt, E. A. *Am. Mineral.* **1998**, *83*, 390.
- 27) Sykora, R. E.; Ok, K. M.; Halasyamani, P. S.; Albrecht-Schmitt, T. E. *J. Am. Chem. Soc.* **2002**, *124*, 1951. b) Shehee, T. C.; Sykora, R. E.; Ok, K. M.; Halasyamani, P. S.; Albrecht-Schmitt, T. E. *Inorg. Chem.* **2003**, *42*, 457. c) Halasyamani, P. S. *Chem. Mater.* **2004**, *16*, 3586 (and references therein). d) Sullens, T. A.; Almond, P. M.; Byrd, J. A.; Beitz, J. V.; Albrecht-Schmitt, T. E. *J. Solid State Chem.* **2006**, *179*, 1181. e) Ok, K. M.; Halasyamani, P. S. *Inorg. Chem.* **2005**, *44*, 9353. Ok, K. M.; Halasyamani, P. S. *Inorg. Chem.* **2005**, *44*, 2263. Ok, K. M.; Halasyamani, P. S. *Angew. Chem., Inter. Ed.* **2004**, *43*, 5489.
- 28) R. E. Sykora, K. M. Ok, P. S. Halasyamani, D. M. Wells, and T. E. Albrecht-Schmitt, *Chem. Mater.* **2002**, *14*, 2741.
- 29) Shannon, R. D. *Acta Crystallogr.* **1976**, *A32*, 751.

Table 1. IR Vibrational Modes for Na₂[UO₂(IO₃)₄(H₂O)] (KBr, cm⁻¹).

UO ₂ ²⁺	IO ₃ ⁻	H ₂ O
903 (ν ₃)	816 (ν)	3290 (ν)
865 (ν ₁)	796 (ν)	3186 (ν)
	786 (ν)	1622 (δ)
	763 (ν)	
	731 (ν)	
	697 (ν)	
	564 (δ)	

Table 2. Crystallographic Data for Na₂[UO₂(IO₃)₄(H₂O)].

Formula	Na ₂ [UO ₂ (IO ₃) ₄ (H ₂ O)]
Formula Mass	1033.63
Color and habit	yellow prism
Space group	<i>C</i> 2 (No. 5)
<i>a</i> (Å)	11.3810(12)
<i>b</i> (Å)	8.0547(8)
<i>c</i> (Å)	7.6515(8)
α (°)	90
β (°)	90.102(2)
γ (°)	90
<i>V</i> (Å ³)	701.42(13)
<i>Z</i>	2
<i>T</i> (K)	193
λ (Å)	0.71073
Maximum 2 θ (deg.)	56.54
ρ_{calcd} (g cm ⁻³)	4.884
$\mu(\text{Mo } K\alpha)$ (cm ⁻¹)	205.13
$R(F)$ for $F_o^2 > 2\sigma(F_o^2)^a$	0.0263
$R_w(F_o^2)^b$	0.0675

^a $R(F) = \sum \|F_o\| - |F_c| / \sum |F_o|$. ^b $R_w(F_o^2) = \left[\sum \left[w(F_o^2 - F_c^2)^2 \right] / \sum wF_o^4 \right]^{1/2}$.

Table 3. Selected Bond Distances (Å) and Angles (°) for Na₂[UO₂(IO₃)₄(H₂O)].

Distances (Å)			
U(1)–O(1) (× 2)	2.302(8)	I(1)–O(1)	1.843(7)
U(1)–O(5) (× 2)	2.345(7)	I(1)–O(2)	1.799(7)
U(1)–O(7) (H ₂ O)	2.450(11)	I(1)–O(3)	1.795(7)
U(1)–O(8) (× 2)	1.787(6)	I(2)–O(4)	1.803(7)
		I(2)–O(5)	1.811(7)
		I(2)–O(6)	1.793(7)
Angles (°)			
O(8)–U(1)–O(8)'	179.2(6)		

Table 4. Cation Effects on the Formation of Uranyl Iodates.

Compound	Crystal Radius of Cation (Å)²⁹	Dimensionality	Ref.
UO ₂ (IO ₃) ₂	n/a	1D	2b
UO ₂ (IO ₃) ₂ (H ₂ O)	n/a	2D	2b
Na ₂ [UO ₂ (IO ₃) ₄ (H ₂ O)]	1.16, 1.32	0D	herein
K[UO ₂ (IO ₃) ₃]	1.65	2D	2j
K ₃ [(UO ₂) ₂ (IO ₃) ₆](IO ₃)·H ₂ O	1.65	1D	2h
K ₂ [(UO ₂) ₃ (IO ₃) ₄ O ₂]	1.65	1D	2f,2g
Rb ₂ [(UO ₂) ₃ (IO ₃) ₄ O ₂]	1.75	1D	2f,2g
Tl ₂ [(UO ₂) ₃ (IO ₃) ₄ O ₂]	1.73	1D	2f,2g
Sr[(UO ₂) ₂ (IO ₃) ₂ O ₂]	1.40	1D	2f,2g
Ba[(UO ₂) ₂ (IO ₃) ₂ O ₂]	1.61	1D	2f,2g
Pb[(UO ₂) ₂ (IO ₃) ₂ O ₂]	1.43	1D	2f,2g
Rb[(UO ₂)(CrO ₄)(IO ₃)(H ₂ O)]	1.75	1D	2e
K ₂ [(UO ₂)(CrO ₄)(IO ₃) ₂]	1.65	1D	2e
Rb ₂ [(UO ₂)(CrO ₄)(IO ₃) ₂]	1.75	1D	2e
Cs ₂ [(UO ₂)(CrO ₄)(IO ₃) ₂]	1.88	1D	2d,2e
K ₂ [(UO ₂)(MoO ₄)(IO ₃) ₂]	1.65	1D	2e
Cs ₂ [(UO ₂) ₃ Cl ₂ (IO ₃)(OH)O ₂]·2H ₂ O	1.92	1D	2c

Figure Captions

Figure 1. A view of the structure of the $[\text{UO}_2(\text{IO}_3)_4(\text{H}_2\text{O})]^{2-}$ anion in $\text{Na}_2[\text{UO}_2(\text{IO}_3)_4(\text{H}_2\text{O})]$, which has imposed two-fold symmetry. 50% probability ellipsoids are depicted.

Figure 2. An illustration of $[\text{UO}_2(\text{IO}_3)_4(\text{H}_2\text{O})]$ units found in $\text{UO}_2(\text{IO}_3)_2(\text{H}_2\text{O})$.

Figure 3. A depiction of the one-dimensional chains of $[\text{UO}_2(\text{IO}_3)_4(\text{H}_2\text{O})]^{2-}$ anions formed through intermolecular hydrogen bonds between the coordinating water molecule and oxo atoms of iodate from adjacent anions. The dashed lines between iodate anions within individual $[\text{UO}_2(\text{IO}_3)_4(\text{H}_2\text{O})]^{2-}$ anions indicate iodate...iodate interactions that orient the iodate anions along the *b* axis. Therefore, cooperative interactions are present for aligning different groups the structure of $\text{Na}_2[\text{UO}_2(\text{IO}_3)_4(\text{H}_2\text{O})]$, where the hydrogen bonding, intermolecular iodate...iodate interactions, and the lone-pair alignment contribute to the short-range and long-range polarity.

Figure 4. a) A view of the distorted dodecahedral environment around Na(1) and b) the distorted octahedral environment around Na(2) in $\text{Na}_2[\text{UO}_2(\text{IO}_3)_4(\text{H}_2\text{O})]$. The environments around the Na^+ cations are consistent with a polar structure.

Figure 5. A packing diagram for $\text{Na}_2[\text{UO}_2(\text{IO}_3)_4(\text{H}_2\text{O})]$.

Figure 6. DSC and TGA thermograms of $\text{Na}_2[\text{UO}_2(\text{IO}_3)_4(\text{H}_2\text{O})]$.

Synopsis

The first molecular uranyl iodate, $[\text{UO}_2(\text{IO}_3)_4(\text{H}_2\text{O})]^{2-}$, has been isolated as its Na^+ salt from a hydrothermal reaction. The $[\text{UO}_2(\text{IO}_3)_4(\text{H}_2\text{O})]^{2-}$ anion contains a UO_2^{2+} cation bound by four monodentate iodate anions and a water molecule. Cooperative interactions of intermolecular hydrogen bonds and iodate...iodate interactions contribute to the alignment of the lone-pair of electrons on the iodate anions to yield a polar structure. Second-harmonic generation experiments demonstrate the frequency doubling of 1064 nm laser light to 532 nm light by $\text{Na}_2[\text{UO}_2(\text{IO}_3)_4(\text{H}_2\text{O})]$.

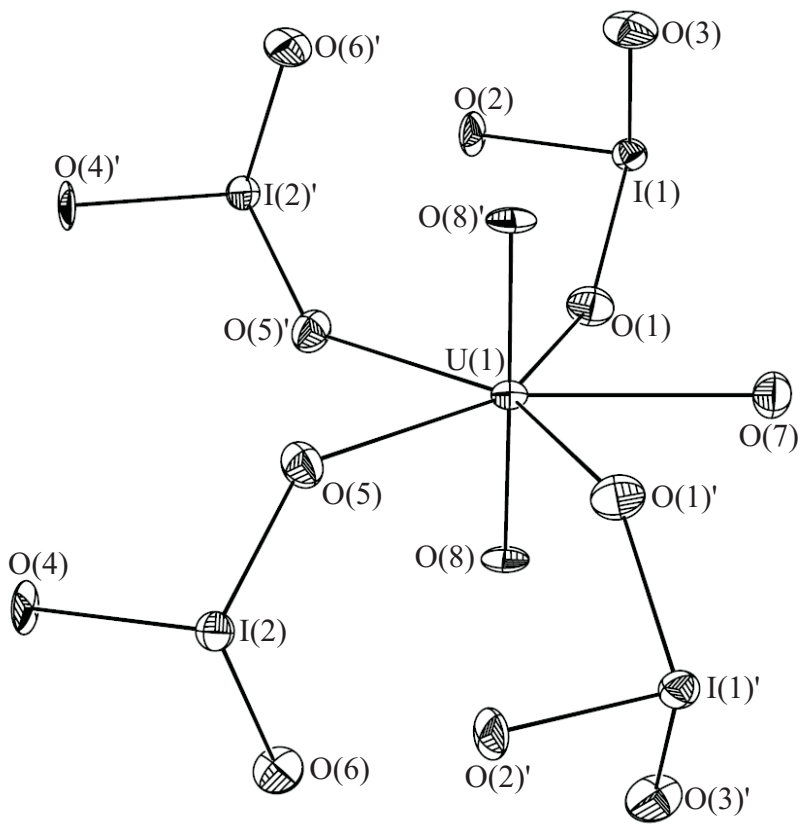


Figure 1.

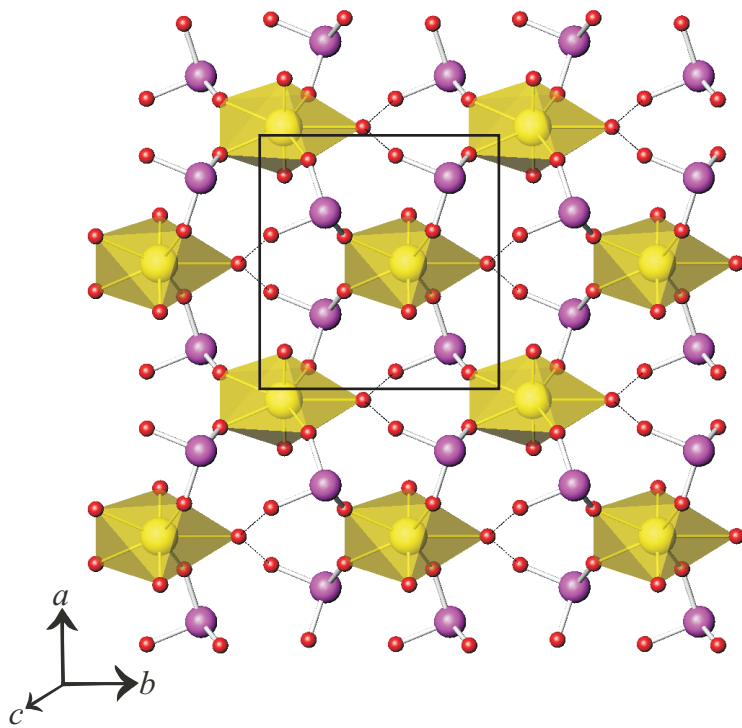


Figure 2.

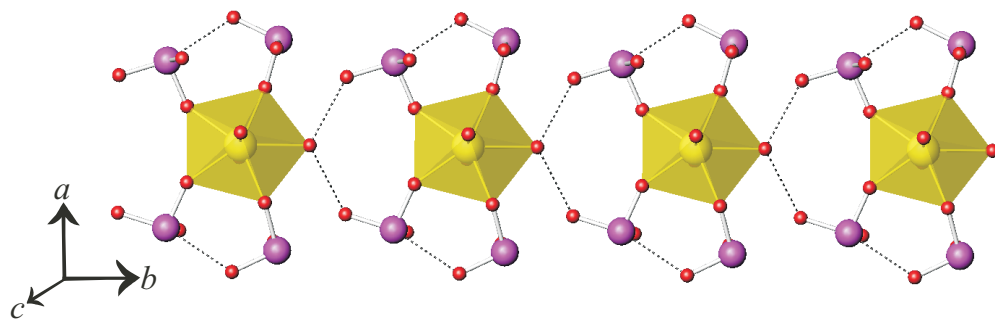


Figure 3.

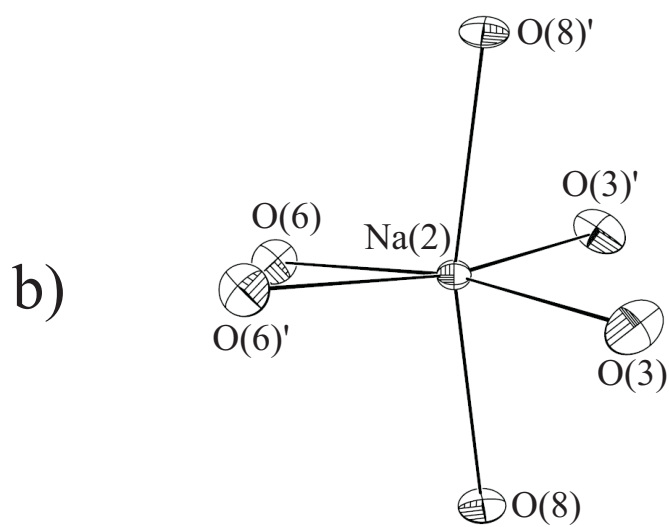
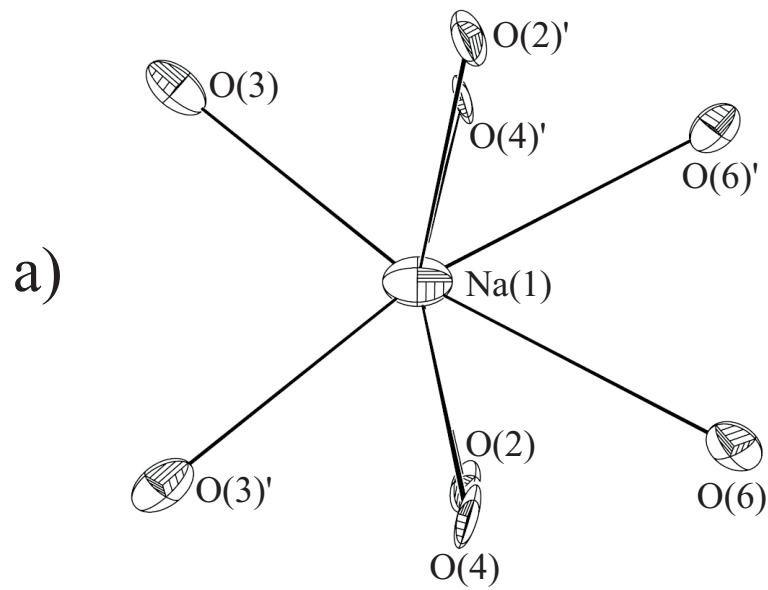


Figure 4.

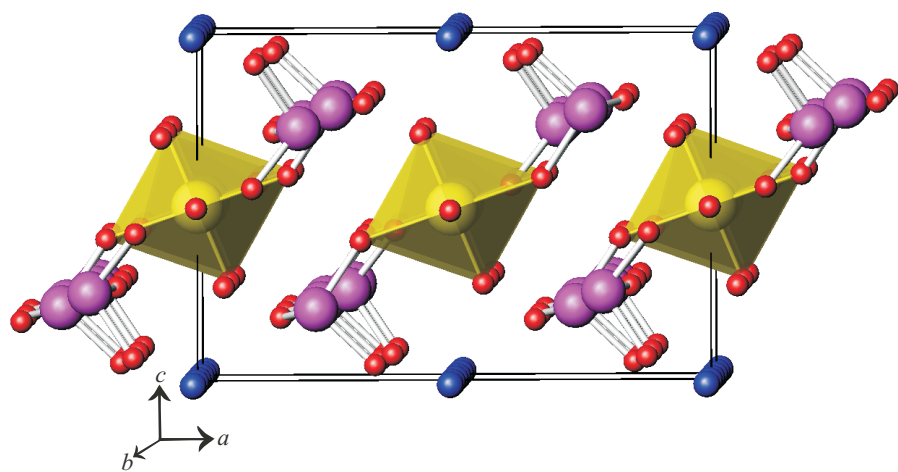


Figure 5.

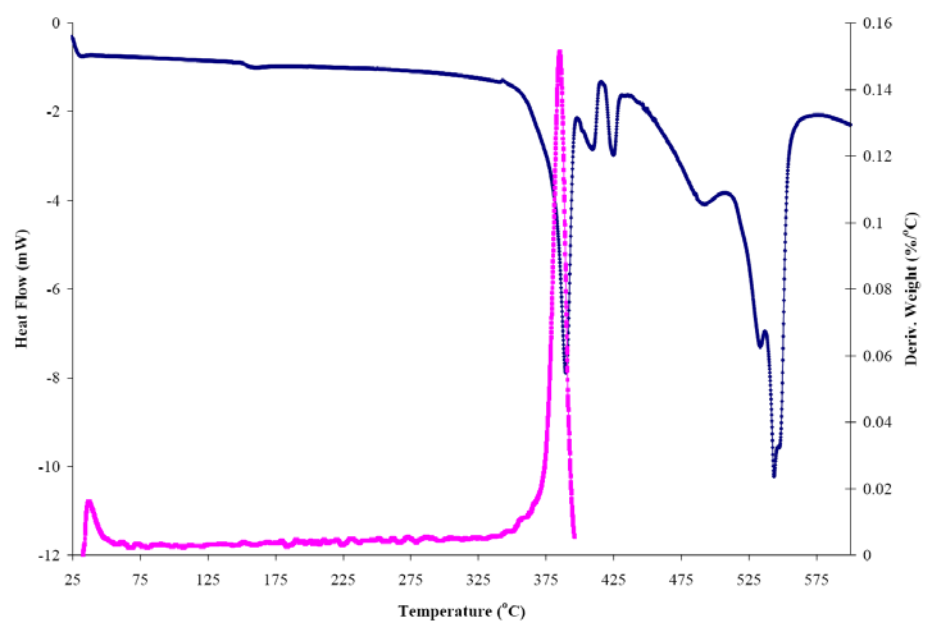


Figure 6.